



**Queensland University of Technology**  
Brisbane Australia

This is the author's version of a work that was submitted/accepted for publication in the following source:

Frost, Ray L. & Keeffe, Eloise C. (2011) The mixed anion mineral parnaute  $\text{Cu}_9[(\text{OH})_{10}(\text{SO}_4)(\text{AsO}_4)_2] \cdot 7\text{H}_2\text{O}$  –a Raman spectroscopic study. *Spectrochimica Acta Part A : Molecular and Biomolecular Spectroscopy*, 81(1), pp. 111-116.

This file was downloaded from: <http://eprints.qut.edu.au/46039/>

© Copyright 2011 Elsevier

this is the author's version of a work that was accepted for publication in <Journal title>. Changes resulting from the publishing process, such as peer review, editing, corrections, structural formatting, and other quality control mechanisms may not be reflected in this document. Changes may have been made to this work since it was submitted for publication. A definitive version was subsequently published in *Spectrochimica Acta Part A : Molecular and Biomolecular Spectroscopy*, 81(10), pp.111-116 DOI: 10.1016/j.saa.2011.05.059

**Notice:** *Changes introduced as a result of publishing processes such as copy-editing and formatting may not be reflected in this document. For a definitive version of this work, please refer to the published source:*

<http://dx.doi.org/10.1016/j.saa.2011.05.059>

**The mixed anion mineral parnaute  $\text{Cu}_9[(\text{OH})_{10}|\text{SO}_4|(\text{AsO}_4)_2]\cdot 7\text{H}_2\text{O}$  –a Raman spectroscopic study**

**Ray L. Frost<sup>\*</sup> and Eloise C. Keeffe**

Inorganic Materials Research Program, School of Physical and Chemical Sciences,  
Queensland University of Technology, GPO Box 2434, Brisbane Queensland 4001,  
Australia.

**Abstract**

The mixed anion mineral parnaute  $\text{Cu}_9[(\text{OH})_{10}|\text{SO}_4|(\text{AsO}_4)_2]\cdot 7\text{H}_2\text{O}$  from two localities namely Cap Garonne Mine, Le Pradet, France and Majuba Hill mine, Pershing County, Nevada, USA has been studied by Raman spectroscopy. The Raman spectrum of the French sample is dominated by an intense band at  $975\text{ cm}^{-1}$  assigned to the  $\nu_1(\text{SO}_4)^{2-}$  symmetric stretching mode and Raman bands at  $1077$  and  $1097\text{ cm}^{-1}$  may be attributed to the  $\nu_3(\text{SO}_4)^{2-}$  antisymmetric stretching mode. Two Raman bands  $1107$  and  $1126\text{ cm}^{-1}$  are assigned to carbonate  $\text{CO}_3^{2-}$  symmetric stretching bands and confirms the presence of carbonate in the structure of parnaute. The comparatively sharp band for the Pershing County mineral at  $976\text{ cm}^{-1}$  is assigned to the  $\nu_1(\text{SO}_4)^{2-}$  symmetric stretching mode and a broad spectral profile centered upon  $1097\text{ cm}^{-1}$  is attributed to the  $\nu_3(\text{SO}_4)^{2-}$  antisymmetric stretching mode. Two intense bands for the Pershing County mineral at  $851$  and  $810\text{ cm}^{-1}$  are assigned to the  $\nu_1(\text{AsO}_4)^{3-}$  symmetric stretching and  $\nu_3(\text{AsO}_4)^{3-}$  antisymmetric stretching modes. Two Raman bands for the French mineral observed at  $725$  and  $777\text{ cm}^{-1}$  are attributed to the  $\nu_3(\text{AsO}_4)^{3-}$  antisymmetric stretching mode. For the French mineral, a low intensity Raman band is observed at  $869\text{ cm}^{-1}$  and is assigned to the  $\nu_1(\text{AsO}_4)^{3-}$  symmetric stretching vibration. Chemical composition of parnaute remains open and the question may be raised is parnaute a solid solution of two or more minerals such as a copper hydroxy-arsenate and a copper hydroxy sulphate.

---

<sup>\*</sup> Author to whom correspondence should be addressed (r.frost@qut.edu.au)

32 **Key words:** parnauite, strashimirite, arsenate minerals, Raman spectroscopy, sulphate,  
33 hydroxyl, molecular water  
34

## INTRODUCTION

Parnauite  $\text{Cu}_9(\text{AsO}_4)_2(\text{SO}_4)(\text{OH})_{10} \cdot 7\text{H}_2\text{O}$  is an uncommon mixed anion mineral containing both sulphate and arsenate [1-3]. Parnauite is a secondary Cu-sulphate-arsenate. The structure of this mineral is not defined [4, 5]. The mineral is probably orthorhombic with point group  $2/m \ 2/m \ 2/m$ . Sometimes the mineral is found with other minerals such as leogangite, goudeyite and strashimirite. Fibrous varieties and crusts may be confused with strashimirite. Another similar formulated mineral is leogangite  $\text{Cu}_{10}(\text{AsO}_4)_4(\text{SO}_4)(\text{OH})_6 \cdot 8\text{H}_2\text{O}$ . Other minerals containing sulphate and arsenate with the copper cation are arsentsumebite, arthurite, chalcophyllite, clinotyrolite, gatrellite and thometzekite. Parnauite is formed as one of supergene product of weathering of primary copper minerals (chalcopyrite, tennantite). Originally, it was found at Majuba Hill Mine, Pershing County, Nevada (U.S.A), in association with chrysocolla and other supergene minerals. Parnauite was found later also on many further localities, however, always as a very rare mineral species. No X-ray single crystal structure data are as yet available. The mineral parnaute contains four vibrational spectroscopically distinct units, namely arsenate, sulphate and hydroxyl units as well as water. The mineral is a mixed anion mineral and is one of a number of mixed anion minerals including minerals of the tsumcorite group and minerals such as peisleyite and strashimirite. Mixed anion minerals are more common than might be expected. Isomorphous substitution for arsenate by other anions such as sulphate results in the mineral parnaute. Chemical composition of parnaute has been open, because some authors assume that this mineral may contain various content of carbonate ions [6].

This research forms part of a comprehensive study of the molecular structure of secondary minerals containing oxy-anions, including uranyl minerals, formed in the oxide zone, using Raman and infrared spectroscopy. Raman spectroscopy has proven most useful for the determination of the molecular structure of minerals [7-16]. The mineral parnaute is an interesting mineral because it is a mixed anion mineral containing both sulphate and arsenate ions as well as hydroxyl ions. As such the Raman spectra will show bands typical of each of these vibrating units. The exact structure of the mineral parnaute is unknown. Raman spectroscopy is a very powerful technique for the determination of molecular structure of minerals when the exact structure from X-ray diffraction is unknown or uncertain. The objective of this research is to compare the Raman properties of parnaute

from Cap Garonne Mine, Le Pradet, France and Majuba Hill mine, Pershing County, Nevada, USA, and relate the Raman spectra to the structure of the mineral.

## **EXPERIMENTAL**

### **Minerals**

The parnauite minerals were supplied by The Mineralogical Research Company. The two parnauite mineral samples originated from parnauite from Cap Garonne Mine, Le Pradet, France (sample A) and Majuba Hill mine, Pershing County, Nevada, USA (sample B). The chemical composition of the mineral has been published [17]. The analysis of the parnauite from Majuba Hill, Nevada, USA, by electron microprobe corresponds to  $\text{Cu}_{8.76}\text{Al}_{0.10}[(\text{AsO}_4)1.43(\text{PO}_4)_{0.43}]_{\Sigma=1.86}(\text{SO}_4)_{0.94}(\text{CO}_3)_{0.19}(\text{OH})_{9.98} \cdot 6.81\text{H}_2\text{O}$ . The mineral analysed as  $\text{Cu}_9(\text{AsO}_4)_2(\text{SO}_4)(\text{OH})_{10} \cdot 7\text{H}_2\text{O}$ . Sample A from Cap Garonne mine, France is associated with cyanotrichite, brochantite, lavendulan, mansfieldite–scorodite, chalcopyrite, cornubite. Sample B from Majuba Hill, Nevada, USA, has paragenetic relationships with the minerals spangolite, chalcophyllite, chenevixite, goudeyite, malachite, azurite brochantite and chrysocolla

### **Raman spectroscopy**

The crystals of parnauite were placed and oriented on the stage of an Olympus BHSM microscope, equipped with 10x and 50x objectives and part of a Renishaw 1000 Raman microscope system, which also includes a monochromator, a filter system and a Charge Coupled Device (CCD). Raman spectra were excited by a HeNe laser (633 nm) at a nominal resolution of  $2\text{ cm}^{-1}$  in the range between 100 and  $4000\text{ cm}^{-1}$ . Details of the experimental procedure have been published. The spatial resolution of the instrument is , 1  $\mu\text{m}$ . Thus if crystals are less than this value, a mixture of crystals will be measured. However the crystals of parnauite used in this experiment were  $> 1\text{ }\mu\text{m}$ . Thus any presence of for example carbonate is therefore assumed to be part of the crystal structure.

Spectral manipulation such as baseline adjustment, smoothing and normalisation were performed using the Spectralcalc software package GRAMS (Galactic Industries Corporation, NH, USA). Band component analysis was undertaken using the Jandel 'Peakfit' software package which enabled the type of fitting function to be selected and allows specific parameters to be fixed or varied accordingly. Band fitting was done using a Lorentz-Gauss cross-product function with the minimum number of component bands used for the fitting process. The Gauss-Lorentz ratio was maintained at values greater than 0.7 and fitting was undertaken until reproducible results were obtained with squared correlations of  $r^2$  greater than 0.995.

## RESULTS AND DISCUSSION

### Raman spectroscopy of the arsenate anion

In aqueous systems, the sulphate anion is of  $T_d$  symmetry and has symmetric stretching mode ( $\nu_1$ ) at  $981\text{ cm}^{-1}$ , the antisymmetric stretching mode ( $\nu_3$ ) at  $1104\text{ cm}^{-1}$ , the symmetric bending mode ( $\nu_2$ ) at  $451\text{ cm}^{-1}$  and the  $\nu_4$  mode at  $613\text{ cm}^{-1}$  [18, 19]. The Raman spectrum of the mineral chalcantite shows a single symmetric stretching mode at  $984.7\text{ cm}^{-1}$ . Two  $\nu_2$  modes are observed at  $463$  and  $445\text{ cm}^{-1}$  and three  $\nu_3$  modes at  $1173$ ,  $1146$  and  $1100\text{ cm}^{-1}$ . The  $\nu_4$  mode is observed as a single band at  $610\text{ cm}^{-1}$ . The arsenate ion,  $(\text{AsO}_4)^{3-}$ , is a tetrahedral unit with  $T_d$  symmetry and exhibit four fundamental vibrations: the symmetric stretching vibration  $\nu_1$  ( $A_1$ ) ( $818\text{ cm}^{-1}$ ), the doubly degenerate bending vibration  $\nu_2$  ( $E$ ) ( $350\text{ cm}^{-1}$ ), the triply degenerate antisymmetric stretching vibration  $\nu_3$  ( $F_2$ ) ( $786\text{ cm}^{-1}$ ), and the triply degenerate bending vibration  $\nu_4$  ( $F_2$ ) ( $398\text{ cm}^{-1}$ ). The  $F_2$  modes are Raman and infrared active, whereas  $A_1$  and  $E$  modes are Raman active only. According to Frost *et al.* the  $\nu_1$  ( $\text{AsO}_4$ ) $^{3-}$  vibration may coincide with the  $\nu_3$  ( $\text{AsO}_4$ ) $^{3-}$  vibration. It should be noted that the wavenumber of the  $\nu_1$  ( $\text{AsO}_4$ ) $^{3-}$  may be greater than that of the  $\nu_3$  ( $\text{AsO}_4$ ) $^{3-}$  which is an inversion of the normal behavior shown by most tetrahedral ions, although such an inversion is not unique [20, 21]. According to Myneni *et al.* [22], the  $T_d$  symmetry of  $(\text{AsO}_4)^{3-}$  unit is rarely preserved in minerals and synthetic compounds, because of its strong affinity to protonate, hydrate, and complex with metal ions. Such chemical interactions reduce  $(\text{AsO}_4)^{3-}$  tetrahedral symmetry to either  $C_{3v}/C_3$  (corner sharing),  $C_{2v}/C_2$  (edge-sharing, bidentate

binuclear), or  $C_1/C_s$  (corner sharing, edge-sharing, bidentate binuclear, multidentate]. This symmetry lowering is connected with activation of all vibrations in infrared and Raman spectra and splitting of doubly and triply degenerate vibrations. Nine normal modes may be Raman and infrared active in the case of the lowest  $C_s$  symmetry [23].

### **Raman spectroscopy of parnauite**

The Raman spectrum of parnauite of samples A and B in the 700 to 1200  $\text{cm}^{-1}$  region is displayed in Figs. 1 and 2. This region includes the symmetric stretching region of both the  $(\text{AsO}_4)^{3-}$  units and the  $(\text{SO}_4)^{2-}$  ions. The Raman spectrum of sample A in this spectral region is dominated by an intense band at 975  $\text{cm}^{-1}$  and is assigned to the  $\nu_1 (\text{SO}_4)^{2-}$  symmetric stretching mode. This band is not so intense for sample B (Fig. 2) and appears significantly broader. In the Raman spectrum of A, four bands are observed at 1077, 1098, 1107 and 1126  $\text{cm}^{-1}$ . The bands centered upon 1077 and 1097  $\text{cm}^{-1}$  may be attributed to the  $\nu_3 (\text{SO}_4)^{2-}$  antisymmetric stretching mode. The two higher wavenumber bands may be assigned to carbonate  $\text{CO}_3^{2-}$  symmetric stretching bands. The presence of these bands confirms the presence of carbonate in the mineral parnauite as first suggested by Kolitsch [6]. For sample B, a Raman band is observed at 1035  $\text{cm}^{-1}$  attributed to the  $\nu_3 (\text{SO}_4)^{2-}$  antisymmetric stretching mode. The broad band at 1135  $\text{cm}^{-1}$  may be ascribed to the carbonate  $\text{CO}_3^{2-}$  antisymmetric stretching mode. In this research, the Raman spectra are taken for an aligned single crystal. The spatial resolution of the instrument is  $\sim 1 \mu\text{m}$  and if crystals are larger than this value as is the case of the measured samples, then a spectrum of parnauite is obtained. If the crystals are  $\ll 1 \mu\text{m}$ , then the spectrum results from the scattering of incident radiation from several crystals. Thus if an impurity such as a carbonate bearing mineral was present, then the spectrum of the sample together with that of carbonate would be determined. Several authors have found that carbonate is present in parnauite minerals [6].

For sample B, a broad envelope of overlapping bands centered upon 851  $\text{cm}^{-1}$  is observed. Band component analysis enables bands to be resolved with two intense bands at 851 and 810  $\text{cm}^{-1}$ . These bands are assigned to the  $\nu_1 (\text{AsO}_4)^{3-}$  symmetric stretching and  $\nu_3 (\text{AsO}_4)^{3-}$  antisymmetric stretching modes, respectively. For sample A, a low intensity Raman band is observed at 869  $\text{cm}^{-1}$  which is assigned to the  $\nu_1 (\text{AsO}_4)^{3-}$  symmetric stretching

vibration. The intensity of the  $(\text{AsO}_4)^{3-}$  is such that the antisymmetric band could not be identified. Two Raman bands are observed at 725 and 777  $\text{cm}^{-1}$  which are not observed in the Raman spectrum of B. These bands may be attributed to hydroxyl deformation modes. An alternative assignment is in terms of the  $\nu_3$   $(\text{AsO}_4)^{3-}$  antisymmetric stretching mode. The observation of multiple bands is attributed to the symmetry reduction of the  $(\text{AsO}_4)^{3-}$  anion as described above.

The Raman spectra of samples A and B in the 300 to 700  $\text{cm}^{-1}$  region are shown in Figs. 3 and 4. The Raman spectra for this spectral region may be contrasted. For sample A, the bands are well defined and component bands may be resolved. For sample B, the spectra are broad and overlap. A set of three bands is observed at 597, 610 and 622  $\text{cm}^{-1}$  and are assigned to the triply degenerate  $\nu_4$   $(\text{SO}_4^{2-})$  bending modes. For the parnauite from Pershing County a set of overlapping bands is observed centered upon 614  $\text{cm}^{-1}$ . Four bands are observed at 600, 614, 620 and 632  $\text{cm}^{-1}$ . The differences in the band positions between samples A and B is quite remarkable. The intense bands of sample A at 451, 482 and 510  $\text{cm}^{-1}$  are attributed to the degenerate  $\nu_4$   $(\text{SO}_4^{2-})$  bending modes. For sample B, a broad spectral profile is observed with component bands resolved at 463, 471 and 512  $\text{cm}^{-1}$ . The bands in the 400 to 500  $\text{cm}^{-1}$  region are assignable to the bending  $\nu_2$  ( $F_2$ ) mode. The most intense band is observed at 482  $\text{cm}^{-1}$  with other bands at 451 and 510  $\text{cm}^{-1}$ . The observation of multiple bands is characteristic of reduced symmetry of the  $\text{AsO}_4$  unit in the crystal. The Raman spectra of kankite in this region show an intense band at 492  $\text{cm}^{-1}$  and similarly pharmacosiderite shows an intense band at 475  $\text{cm}^{-1}$ . For clinotyrolite, an intense band is observed at 493  $\text{cm}^{-1}$  with shoulders at 462 and 505  $\text{cm}^{-1}$ . The intense bands at 366 and 397  $\text{cm}^{-1}$  in the Raman spectrum of sample A, are due to the  $(\text{AsO}_4)^{3-}$   $\nu_2$  (E) bending mode. For sample B, a broad band at 380  $\text{cm}^{-1}$  is observed. The band at 319  $\text{cm}^{-1}$  is attributed to  $(\text{AsO}_4)^{3-}$   $\nu_4$  (E) bending mode. The band is observed at 311  $\text{cm}^{-1}$  for sample B. A significant number of bands is observed in the 100 to 300  $\text{cm}^{-1}$  region for sample A (Figure 5). Raman bands are observed at 107, 120, 131, 141, 150, 158, 170, 188, 197, 244 and 263  $\text{cm}^{-1}$ . In contrast the spectral profile is broad in the Raman spectrum of sample B. Raman bands are observed at 111, 148 (broad), 176 (broad), 225, 240, 264 and 274  $\text{cm}^{-1}$  (Figure 6). It is considered that the bands at around 244 and 263  $\text{cm}^{-1}$  are related to water hydrogen bonding.



The Raman spectrum of samples A and B parnaute in the 3100 to 3500  $\text{cm}^{-1}$  region are shown in Figures 7 and 8. Three distinct Raman bands are observed for sample A at 3255, 3372 and 3410  $\text{cm}^{-1}$  with a component band at 3402  $\text{cm}^{-1}$ . The first band at 3255  $\text{cm}^{-1}$  is attributed to water OH stretching bands. The two bands at 3372 and 3410  $\text{cm}^{-1}$  are assigned to the hydroxyl stretching vibrations. Studies have shown a strong correlation between OH stretching frequencies and both the O $\cdots$ O bond distances and the H $\cdots$ O hydrogen bond distances. The elegant work of Libowitzky<sup>43</sup> showed that a regression function can be employed relating the above correlations with regression coefficients better than 0.96<sup>43</sup>. The function is  $\nu_1 = (3592 - 304) \times 109^{\frac{-d(O-O)}{0.1321}} \text{ cm}^{-1}$ . Two types of OH units are identified in the structure and the known hydrogen bond distances used to predict the hydroxyl stretching frequencies. Thus if we calculate the hydrogen bond distances using the Libowitzky type formula, the 3410  $\text{cm}^{-1}$  band provide a hydrogen bond distance of 2.805(3) Å, 3372  $\text{cm}^{-1}$  gives 2.780(2) Å, 3255  $\text{cm}^{-1}$  gives 2.723(9) Å. The spectrum of parnaute may be divided into two groups of OH stretching wavenumbers: namely 3500–3700  $\text{cm}^{-1}$  and 2900–3500  $\text{cm}^{-1}$ . This distinction suggests that the strength of the hydrogen bonds as measured by the hydrogen bond distances can also be divided into two groups. An arbitrary cut-off point may be 2.74 Å based upon the wavenumber 3300  $\text{cm}^{-1}$ . The hydrogen bond distances 2.805(3) Å may be described as weak hydrogen bonding and the bond distances of 2.780(2) and 2.723(9) Å as slightly stronger hydrogen bonds. Thus by using the position of the bands in the Raman spectrum, an estimate of the hydrogen bond distances can be made. Such values are difficult to obtain from single crystal X-ray diffraction data. Hydrogen bond distances can be obtained from neutron diffraction data but such studies are very rare.

Recently the Raman spectrum of parnaute from Slovak Republic was published (JRS in press). Three bands for the Slovak parnaute which are attributed to OH stretching vibrations are observed at 3348, 3494 and 3566  $\text{cm}^{-1}$ . The sharp band at 3566  $\text{cm}^{-1}$  is assigned to the OH stretching vibration of the hydroxyl units. The two bands at 3348 and 3494  $\text{cm}^{-1}$  are assigned to water stretching modes. Hydrogen plays an extremely important role in the structure and chemistry of oxysalt minerals such as for mixed arsenate sulphates including parnaute and peisleyite [24]. The presence of water adds to the stability of the oxysalt. [25] For any crystal structure the structural unit may be defined as the strongly bonded part of the unit. Structural units are linked together by interstitial species such as

univalent and divalent cations and by water groups that are involved in much weaker bonding.

## CONCLUSIONS

Raman spectroscopy has been used to characterise the molecular structure of the mineral parnaute  $\text{Cu}_9(\text{AsO}_4)_2(\text{SO}_4)(\text{OH})_{10} \cdot 7\text{H}_2\text{O}$ . Characteristic Raman bands of the  $(\text{AsO}_4)^{3-}$  stretching and bending vibrations were identified and described. Raman bands attributable to the OH stretching vibrations of water and hydroxyl units were analysed.

Considerable differences in the Raman spectra of the two parnaute minerals from the two localities Cap Garonne Mine, Le Pradet, France and Majuba Hill mine, Pershing County, Nevada, USA are observed and reported. The crystal structure of parnaute remains unsolved. Raman spectroscopy proves the presence of carbonate anion in the mineral structure. The question of the exact nature of the mineral parnaute remains somewhat unanswered. Chemical composition of parnaute remains open, because some authors assume that this mineral may contain various content of carbonate ions [6].

## Acknowledgments

The financial and infra-structure support of the Queensland University of Technology, Inorganic Materials Research Program is gratefully acknowledged. The Australian Research Council (ARC) is thanked for funding the instrumentation.

## 263 REFERENCES

- 264 [1] L. Lai, Y. Li, N. Shi, *Yanshi Kuangwuxue Zazhi* 16 (1997) 50-55.
- 265 [2] H. Sarp, J. Deferne, B.W. Liebich, *Arch. Sc.* 31 (1978) 213-217.
- 266 [3] W.S. Wise, *Amer. Min.* 63 (1978) 704-708.
- 267 [4] H. Sarp, J. Deferne, B.W. Liebich, 31 (1978) 213-217.
- 268 [5] W.S. Wise, 63 (1978) 704-708.
- 269 [6] U. Kolitsch, *Aufschluss* 48 (1997) 65-91.
- 270 [7] S. Bahfenne, R.L. Frost, *Spectrochim. Acta*, A74 (2009) 100-103.
- 271 [8] S. Bahfenne, R.L. Frost, *Spectrochim. Acta*, A74 (2009) 625-628.
- 272 [9] R.L. Frost, *Spectrochim. Acta*, A71 (2009) 1788-1794.
- 273 [10] R.L. Frost, *Spectrochim. Acta*, A72 (2009) 903-906.
- 274 [11] R.L. Frost, S. Bahfenne, J. Graham, *Spectrochim. Acta*, A71 (2009) 1610-1616.
- 275 [12] R.L. Frost, J. Cejka, *Spectrochim. Acta*, A 71 (2009) 1959-1963.
- 276 [13] R.L. Frost, J. Cejka, M.J. Dickfos, *Spectrochim. Acta*, A71 (2009) 1799-1803.
- 277 [14] R.L. Frost, M.J. Dickfos, *Spectrochim. Acta*, A72 (2009) 445-448.
- 278 [15] R.L. Frost, M.J. Dickfos, E.C. Keeffe, *Spectrochim. Acta*, A71 (2009) 1663-1666.
- 279 [16] R.L. Frost, M.J. Dickfos, E.C. Keeffe, *Spectrochim. Acta*, A71 (2009) 1512-1515.
- 280 [17] J.W. Anthony, R.A. Bideaux, K.W. Bladh, M.C. Nichols, *Handbook of Mineralogy*
- 281 IV, Arsenates, phosphates, vanadates., Mineral Data Publishing, Tucson, Arizona
- 282 2000.
- 283 [18] R.L. Frost, J.T. Kloprogge, *Neues Jahrb. Mineral., Monatsh.* (2001) 27-40.
- 284 [19] W. Martens, R.L. Frost, J.T. Kloprogge, P.A. Williams, *J. Raman Spectros.* 34 (2003)
- 285 145-151.
- 286 [20] F.K. Vansant, B.J.V.d. Veken, H.O. Desseyn, *J. Mol. Struct.* 15 (1973) 425-437.
- 287 [21] R.H. Busey, O.L. Keller, *J. Chem. Phys.* 41 (1964) 215-225.
- 288 [22] S.C.B. Myneni, S.J. Traina, G.A. Waychunas, T.J. Logan, *Geochim. Cosmochim.*
- 289 *Acta* 62 (1998) 3285-3300.
- 290 [23] S.D. Ross, in: V.C. Farmer (Ed.), *The infrared spectra of minerals*
- 291 Mineralogical Society, London 1974.
- 292 [24] D.M.C. Huminicki, F.C. Hawthorne, *Rev. Min. Geochem.* 48 (2002) 123-325.
- 293 [25] F.C. Hawthorne, *Zeit. Krist.* 201 (1992) 183-206.

294

295

296    **List of Figures**

297    Figure 1 Raman spectrum of parnauite (sample A) in the 700 to 1200  $\text{cm}^{-1}$  region.

298    Figure 2 Raman spectrum of parnauite (sample B) in the 700 to 1200  $\text{cm}^{-1}$  region.

299    Figure 3 Raman spectrum of parnauite (sample A) in the 300 to 700  $\text{cm}^{-1}$  region.

300    Figure 4 Raman spectrum of parnauite (sample B) in the 300 to 700  $\text{cm}^{-1}$  region.

301    Figure 5 Raman spectrum of parnauite (sample A) in the 100 to 300  $\text{cm}^{-1}$  region.

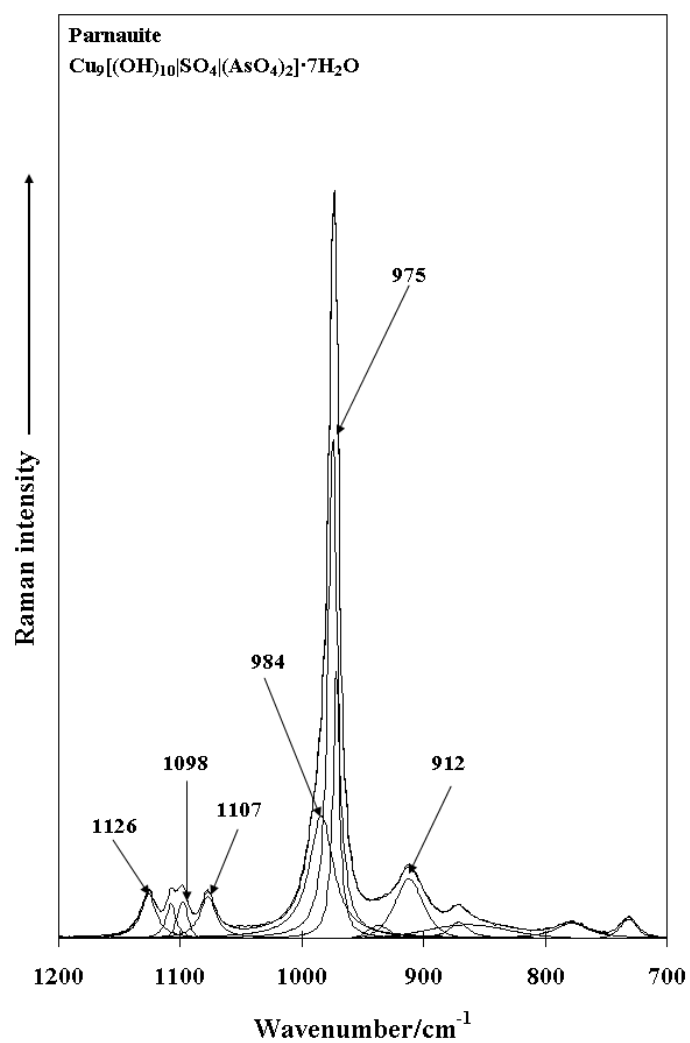
302    Figure 6 Raman spectrum of parnauite (sample B) in the 100 to 300  $\text{cm}^{-1}$  region.

303    Figure 7 Raman spectrum of parnauite (sample A) in the 3100 to 3500  $\text{cm}^{-1}$  region.

304    Figure 8 Raman spectrum of parnauite (sample B) in the 3200 to 3700  $\text{cm}^{-1}$  region.

305

306



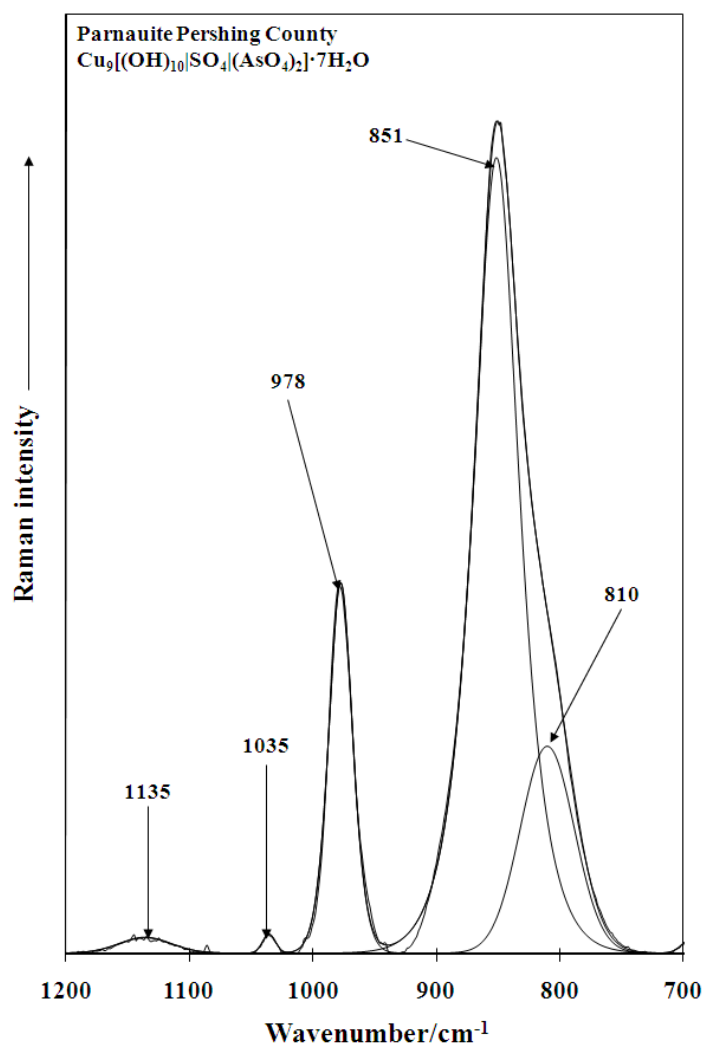
307

308

309 **Figure 1**

310

311



312

313

314 **Figure 2**

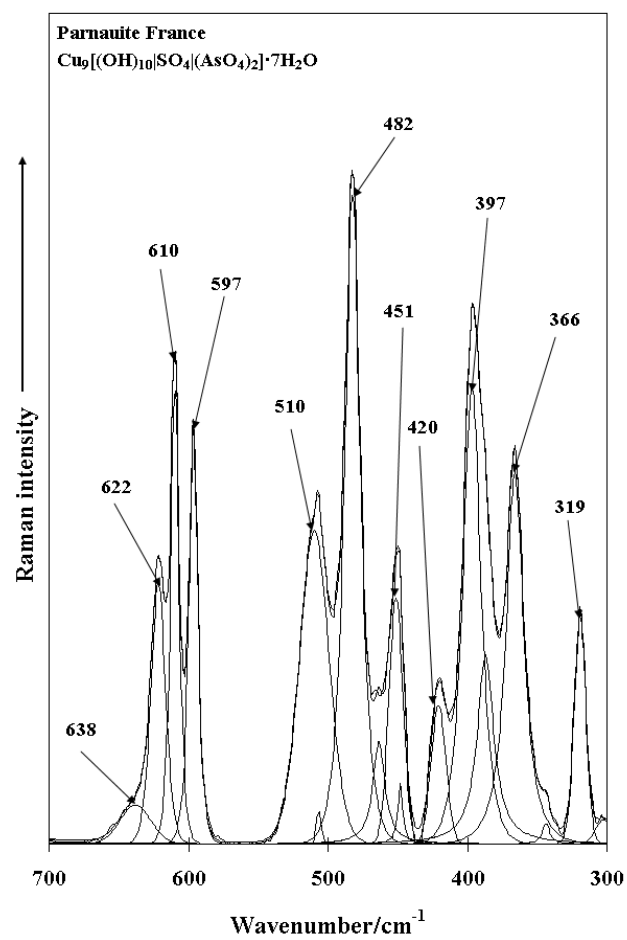


**Figure 3**

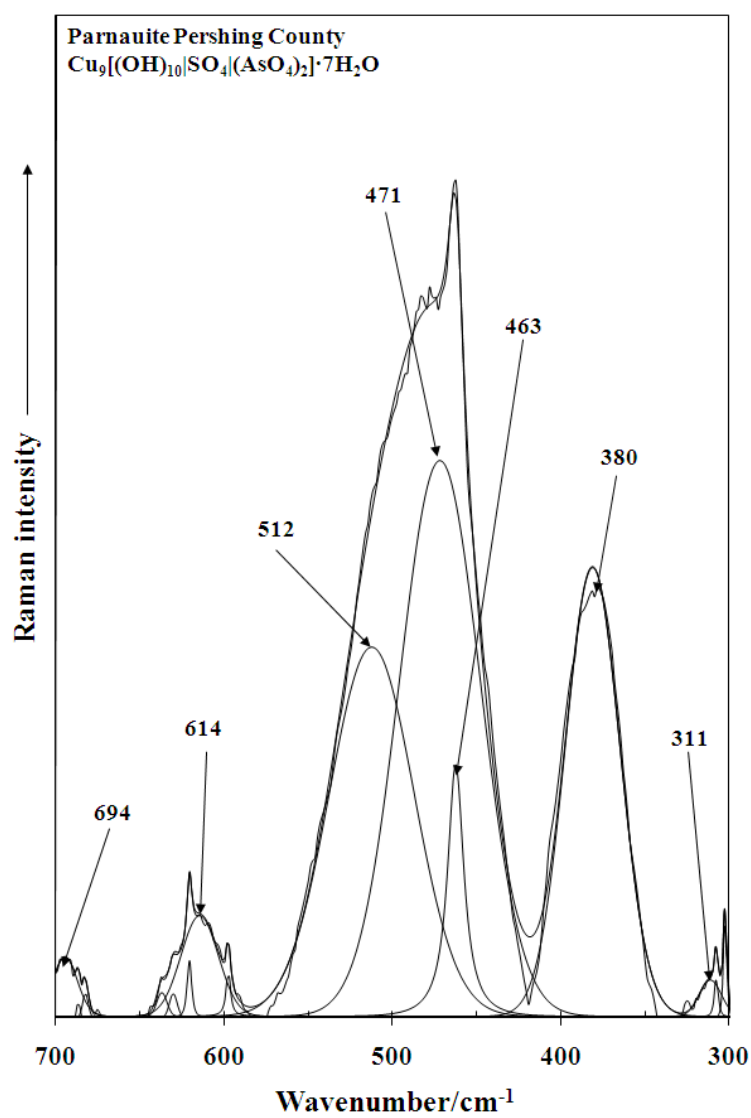


**Figure 4**



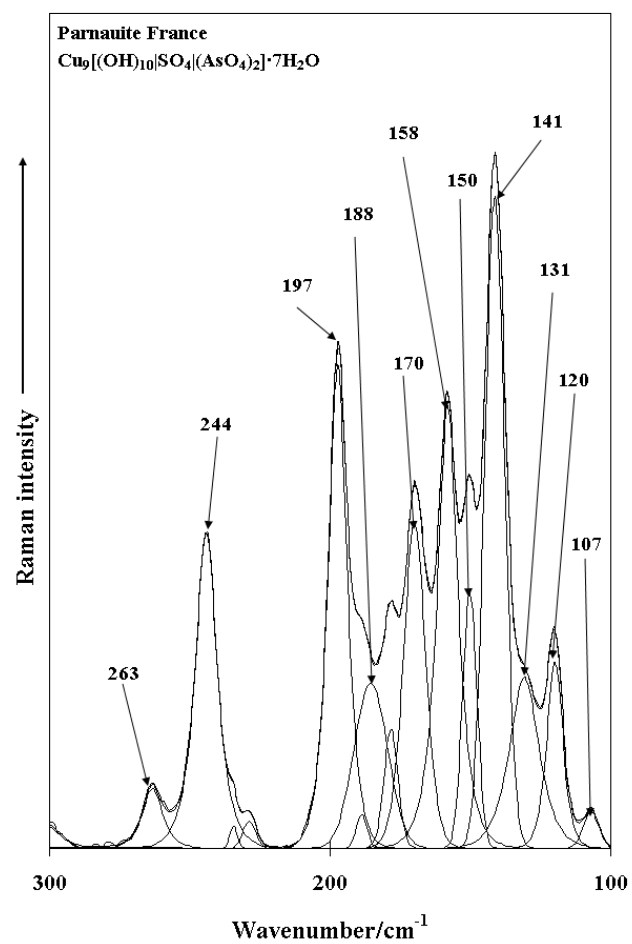
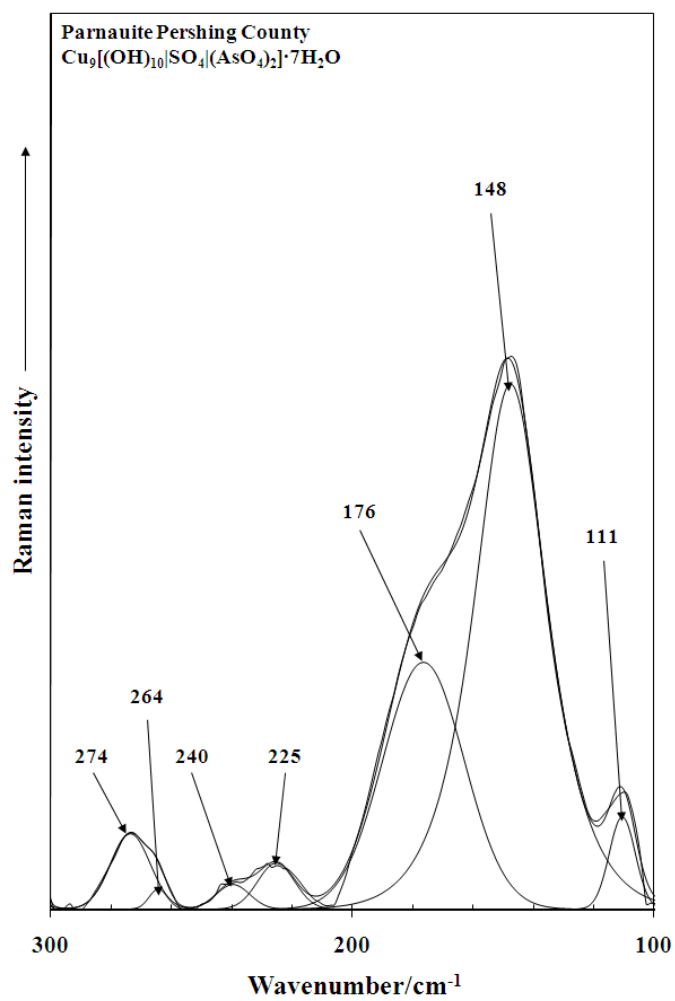


**Figure 5**



328

329

330 **Figure 6**

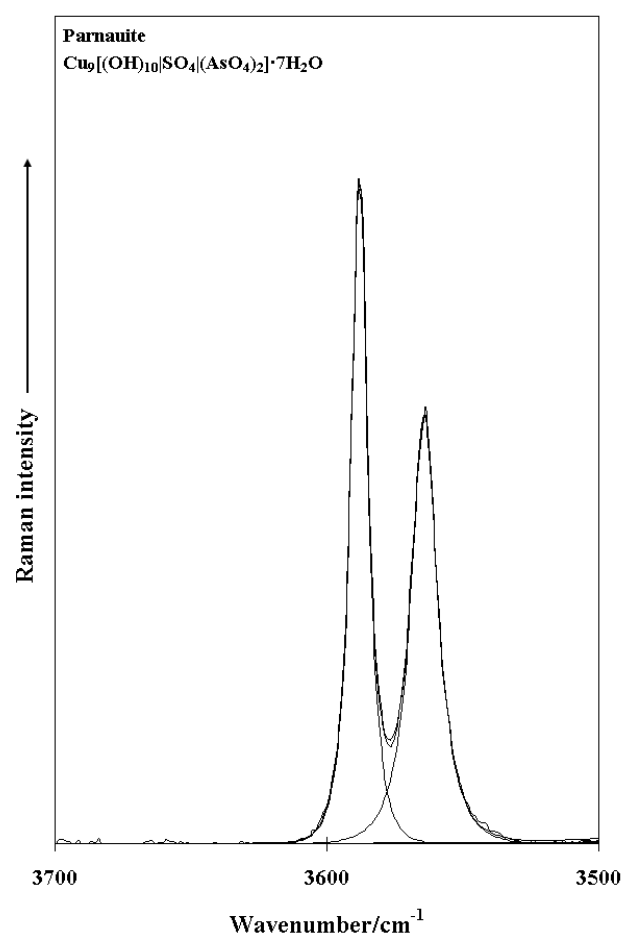


**Figure 7**

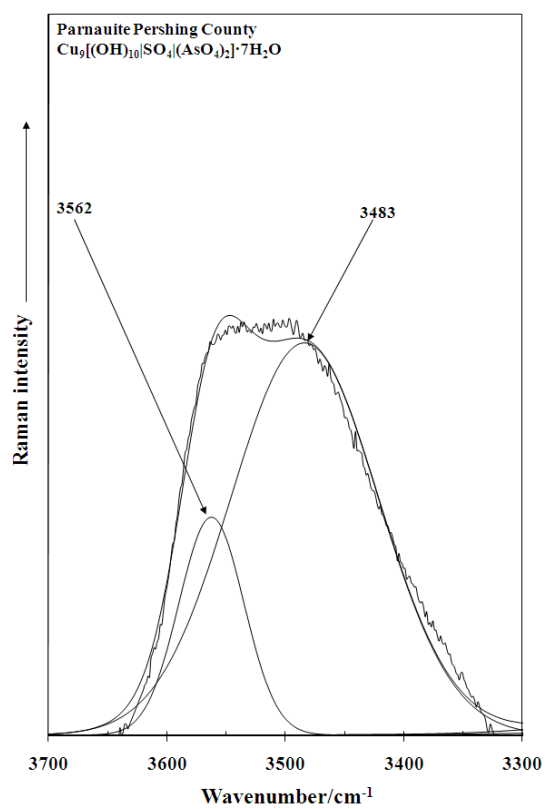


**Figure 8**